Biochimica et Biophysica Acta, 981 (1989) 326–336
Elsevier

BBA 74437

Pump current and Na^+/K^+ coupling ratio of Na^+/K^+-ATPase in reconstituted lipid vesicles

R.J. Clarke *, H.-J. Apell and P. Läuger

Department of Biology, University of Konstanz, Konstanz (F.R.G.)

(Received 20 January 1989)

Key words: ATPase, Na^+/K^+-; Reconstituted lipid vesicle; Ion flux; Pump current; Coupling ratio

A method is described for studying the coupling ratio of the Na^+/K^+ pump, i.e., the ratio of pump-mediated fluxes of Na^+ and K^+, in a reconstituted system. The method is based on the comparison of the pump-generated current with the rate of K^+ transport. Na^+/K^+-ATPase from kidney is incorporated into the membrane of artificial lipid vesicles; ATPase molecules with outward-oriented ATP-binding site are activated by addition of ATP to the medium. Using oxonol VI as a potential-sensitive dye for measuring transmembrane voltage, the pump current is determined from the change of voltage with time t. In a second set of experiments, the membrane is made selectively K^+-permeable by addition of valinomycin, so that the membrane voltage U is equal to the Nernst potential of K^+. Under this condition, dU/dt reflects the change of intravesicular K^+ concentration and thus the flux of K^+. Values of the Na^+/K^+ coupling ratio determined in this way are close to 1.5 in the experimental range (10–75 mM) of extravesicular (cytoplasmic) Na^+ concentrations.

Introduction

The Na^+/K^+ pump in the plasma membrane of animal cells utilizes free energy derived from ATP hydrolysis for extrusion of sodium and uptake of potassium [1–7]. In most systems studied so far, active ion transport mediated by the Na^+/K^+ pump is associated with net inward movement of positive charge [8–11], indicating that the Na^+/K^+ coupling ratio exceeds unity. The coupling ratio is defined as the ratio of the pump-mediated net fluxes, $J_{N,p}$ and $J_{K,p}$, of sodium and potassium. Several investigations have shown that in erythrocytes the coupling ratio is close to 3:2 at physiological ion concentrations [12–16,78]. In other preparations, such as squid giant axon [17–22], muscle fibres [23–34] and epithelia [35,36], the interpretation of the experimental results is less clear, and it is possible that the coupling ratio varies with the ionic conditions. A variable coupling ratio may be expected, for instance, when the pump is able to accept Na^+ instead of K^+ in part of the catalytic cycle. In fact, in the absence of K^+ and in the presence of Na^+ in the extracellular medium, the pump carries out ATP-driven (net) extrusion of Na^+, albeit a low rate [37–40]. This transport mode (which corresponds to a nominally infinite Na^+/K^+ coupling ratio) probably results from a 'potassium-like' effect of sodium at the extracellular ion-binding sites [6]. Conversely, it is feasible that a low intracellular Na^+ concentration, transport cycles occasionally occur in which the protein undergoes the $E_1 \rightarrow E_2$ conformational transition with less than three Na^+ ions bound. A decrease of Na^+/K^+ coupling ratio at low Na^+ concentrations has been observed with membrane vesicles derived from erythrocytes [79].

For investigating the Na^+/K^+ pump, reconstituted lipid vesicles [40–47] offer distinct advantages compared to intact cells which always contain additional transport pathways for Na^+ and K^+. Most ion flux studies with reconstituted vesicles have been done in the past using radioactive isotopes. The common version of the isotope method requires separation of the vesicles from the external medium by filtration or gel chromatography. Since the time resolution of this technique is of the order of seconds [49], an accurate determination of initial transport rates is difficult. A rapid sampling method based on pressure filtration has been developed by Forbush [50]. This technique yields sampling times of the order of 10 ms, but requires high pump densities in the membrane which are not easily achieved with reconstituted vesicles.

* Present address: School of Chemical Sciences, University of East Anglia, Norwich NR4 7TJ, U.K.

Correspondence: H.-J. Apell, Department of Biology, University of Konstanz, D-7750 Konstanz, F.R.G.

A fast and sensitive method for studying pumping rates in reconstituted vesicles consists in recording optical signals associated with ion fluxes [51–55]. In the following, we describe experiments in which the time-course of transmembrane voltage U built-up by the pump is monitored using the potential-sensitive fluorescent dye oxonol VI [53]. From the time-derivative of U and from the electrical capacitance of the membrane, the initial value of the pumping current I_p may be obtained [55]. In addition to I_p, the net pump-mediated potassium flux $J_{K,p}$ is determined in parallel experiments by measuring the valinomycin-induced Nernst potential for K^+ [51]. By comparison of $J_{K,p}$ and $I_p \propto (J_{N,p} - J_{K,p})$, the fluxes $J_{N,p}$ and $J_{K,p}$ of Na^+ and K^+ may be obtained separately.

Materials and Methods

Materials

Dioleoylphosphatidylcholine was obtained from Avanti Polar Lipids (Birmingham, AL, U.S.A.), oxonol VI (bis(3-propyl-5-oxoisooxazol-4-yl)pentamethine oxonol) was from Molecular Probes (Junction City, OR, U.S.A.), ATP (Sonderqualität) and valinomycin from Boehringer-Mannheim, vanadate from Ventron (Karlsruhe, F.R.G.). The phospholipid contents were determined by the Phospholipid B test from Wako Pure Chemical Industries, Ltd. (Osaka, Japan). Choline sulfate was prepared from choline hydroxide by titration with H_2SO_4. All other reagents were obtained from Merck (analytical grade) (Darmstadt, F.R.G.). Dialysis tubing was purchased from Serva (Heidelberg, F.R.G.).

Enzyme preparation

Na^+/K^+-ATPase was prepared from outer medulla of rabbit kidneys using procedure C of Jørgensen [56], as described previously [51,57]. This method yields purified enzyme in the form of membrane fragments containing about 0.6 mg phospholipid and 0.2 mg cholesterol per mg protein [5,56]. The specific activity was in the range of 1700–2100 μmol P_i per h per mg protein at 37°C.

Preparation of reconstituted vesicles

The enzyme was solubilized [51] in a solution of 23 mM sodium cholate in 'buffer H' (30 mM imidazole, 1 mM L-cysteine, 1 mM EDTA and 5 mM $MgSO_4$; the pH was adjusted to 7.2 with H_2SO_4). The enzyme solubilizate was mixed with dioleoylphosphatidylcholine solubilized in cholate buffer [51]. 200 μl of the mixture (10 mg lipid and about 0.6 mg protein per ml) were transfered to 7-mm dialysis tubing and were dialysed for 60 h at 4°C against buffer H containing various concentrations of Na_2SO_4, K_2SO_4 and choline sulfate. The resulting vesicles had an average diameter of 96 nm ± 10 nm [58]. The average number of pump molecules with outward oriented ATP-binding sites, as determined by the indocyanine method [51], was about $n = 4.5$.

Fluorescence measurements

Fluorescence experiments were carried out in a Perkin Elmer 650-40 fluorescence spectrophotometer. The thermostated cuvette holder was equipped with a magnetic stirrer. The excitation wavelength was set to 580 nm (slit width 20 nm) and the emission wavelength to 660 nm (slit width 20 nm). The oxonol VI stock solution contained 0.03 mM dye in ethanol/water (1 : 9, v/v). 1 μl of this solution were added to 1 ml of the medium in the cuvette to get a final (total) oxonol concentration of 30 nM.

The cuvette was filled with 1 ml buffer and equilibrated in the thermostated cuvette holder to the desired temperature. After measuring the background fluorescence, oxonol VI was added. After the fluorescence signal was constant, an aliquot of the vesicle suspension was added. Fluorescence changes, ΔF, caused by additions of reagents were determined as relative changes with respect to the fluroescence level, F_0, prior to the addition. The fluorescence signals were corrected for the small dilution effect which was determined separately by adding a known amount of buffer solution. If not otherwise stated, the experiments were carried out at 22°C.

Theory

Time-course of transmembrane voltage after addition of ATP to the medium

We consider a vesicle of membrane area A, containing n pump molecules with outward-facing ATP binding sites (Fig. 1). Addition of ATP to the medium generates a pump current I_p which is given by

$$I_p = e_0(J_{N,p} + J_{K,p}) \tag{1}$$

e_0 is the elementary charge, and $J_{N,p}$ and $J_{K,p}$ are the pump-mediated fluxes of Na^+ and K^+; $J_{N,p}$ and $J_{K,p}$ are referred to a single vesicle and are taken to be positive for outward translocation.

If the pump has ν transport sites for Na^+ and κ transport sites for K^+, and if in a turnover of the pump the sodium and potassium sites are always fully occupied, then the relations

$$J_{N,p} = -\nu n v; \qquad J_{K,p} = \kappa n v \tag{2}$$

hold, where n is the number of outward-oriented pump molecules per vesicle and v is the turnover rate. In general, however, the coupling ratio $\rho_{NK} \equiv -J_{N,p}/J_{K,p}$ has to be distinguished from the stoichiometric ratio $\sigma_{NK} \equiv \nu/\kappa$. σ_{NK} has a fixed value which is determined

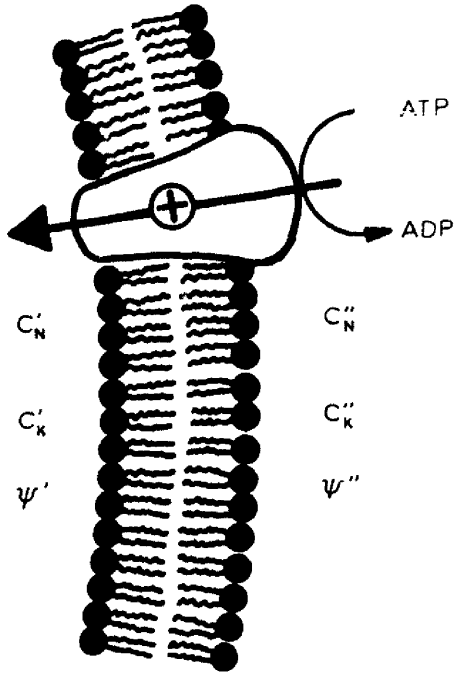

Fig. 1. Na^+/K^+-ATPase molecule with outward-facing ATP-binding site embedded in the membrane of a lipid vesicle. c'_N and c'_K are the intravesicular concentrations of Na^+ and K^+, respectively, c''_N and c''_K are the external concentrations and ψ' and ψ'' are the electrical potentials.

by the structure of the transport protein; in the case of the Na^+/K^+ pump from erythrocytes it is well established that σ_{NK} is equal to 3/2 [6]. The coupling ratio ρ_{NK}, on the other hand, may vary according to the experimental conditions, as discussed in the Introduction.

The total current I through the vesicle membrane contains, in addition to I_p, contributions from leakage pathways. Denoting the passive (leakage) fluxes of Na^+ and K^+ by $J_{N,l}$ and $J_{K,l}$, respectively, the transmembrane current I may be represented by

$$I = I_p + e_0(J_{N,l} + J_{K,l}) + \lambda AU \tag{3}$$

λ is the specific membrane conductance (S/m^2) accounting for contributions of ionic species other than Na^+ and K^+, A the membrane area and $U \equiv \psi' - \psi''$ the transmembrane voltage. λ may be considered as a voltage-independent constant. The dependence of $J_{N,l}$ and $J_{K,l}$ on ion concentration and voltage may be described by the Goldman relation [59]

$$J_{N,l} = P_N A u \frac{c'_N \exp(u) - c''_N}{\exp(u) - 1} \tag{4}$$

$$J_{K,l} = P_K A u \frac{c'_K \exp(u) - c''_K}{\exp(u) - 1} \tag{5}$$

$$u \equiv \frac{\psi' - \psi''}{RT/F} = \frac{U}{RT/F} \tag{6}$$

(compare Fig. 1). P_N and P_K are the permeability coefficients of Na^+ and K^+, R is the gas constant, T the absolute temperature and F, here the Faraday constant. c'_N, c''_N, c'_K and c''_K are expressed as number of particles per unit volume (′ intravesicular, ″ extravesicular).

The rate of change of transmembrane voltage U is proportional to the net current I and inversely proportional to the electric capacitance AC_m of the membrane (C_m is the membrane capacitance per unit area)

$$\frac{dU}{dt} = \frac{-I}{AC_m} \tag{7}$$

The rate of change of the intravesicular concentrations of Na^+ and K^+ is given by the sum of pump-mediated and leakage fluxes

$$-V_i \frac{dc'_N}{dt} = J_{N,p} + J_{N,l} \tag{8}$$

$$-V_i \frac{dc'_K}{dt} = J_{K,p} + J_{K,l} \tag{9}$$

V_i is the volume of the intravesicular aqueous space. The volume V_e of the extravesicular space is assumed to be large, so that the concentrations c''_K and c''_N remain virtually constant during the experiment. Eqns. 1–9 yield the following differential equations for the three variables $u(t)$, $c'_N(t)$ and $c'_K(t)$

$$-\frac{du}{dt} = Q\left[J_{N,p} + J_{K,p} + AP_N u \frac{c'_N \exp(u) - c''_N}{\exp(u) - 1} + AP_K u \frac{c'_K \exp(u) - c''_K}{\exp(u) - 1}\right] + \frac{\lambda u}{C_m} \tag{10}$$

$$-V_i \frac{dc'_N}{dt} = J_{N,p} + AP_N u \frac{c'_N \exp(u) - c''_N}{\exp(u) - 1} \tag{11}$$

$$-V_i \frac{dc'_K}{dt} = J_{K,p} + AP_K u \frac{c'_K \exp(u) - c''_K}{\exp(u) - 1} \tag{12}$$

$$Q \equiv e_0 F/RTAC_m \tag{13}$$

$1/Q$ is the number of elementary charges required to charge the membrane capacitance AC_m to the voltage $RT/F \cong 25$ mV; for a spherical vesicle of radius $r = 50$ nm and with a specific membrane capacitance $C_m \approx 1$ $\mu F/cm^2$, the relation $1/Q \approx 49$ holds.

The meaning of Eqns. 10–12 may be illustrated by considering numerical solutions. In the example represented in Fig. 2, the system is assumed to be symmetric at the beginning ($c'_N = c''_N$, $c'_K = c''_K$ and $u = 0$ at $t \leq 0$). At time $t = 0$, pumps are activated by addition of ATP to the medium. The set of curves in Fig. 2 corresponds to experiments in which the permeability coefficients P_K and P_N are varied by varying the aqueous valinomycin concentration c^a_{val}, assuming that P_K and P_N are

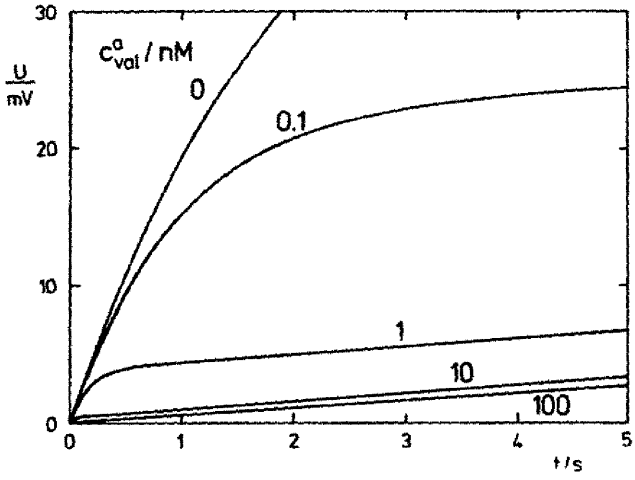

Fig. 2. Predicted time-course of transmembrane voltage U after pump activation at $t = 0$ for different values of the aqueous valinomycin concentration c^a_{val}. $U(t)$ was obtained by numerical integration of Eqns. 10–12 for spherical vesicles of radius $r_i = 45$ nm and membrane thickness $d = 4$ nm, using the following parameter values: $J_{N,p} = -3\ nv$, $J_{K,p} = 2\ nv$, $n = 5$, $v = 121\ s^{-1}$, $C_m = 1\ \mu F/cm^2$, $\lambda = 0$, $T = 293$ K, $A = 4\pi(r_i + d)$, $V_i = (4\pi/3)r_i^3$, $a_K = 60\ cm \cdot M^{-1} \cdot s^{-1}$, $a_N = 0.09\ cm \cdot M^{-1} \cdot s^{-1}$, $b_K = 10^{-9}\ cm \cdot s^{-1}$, $b_N = 8 \cdot 10^{-10}\ cm \cdot s^{-1}$. The initial conditions were chosen to be $c'_K = c''_K = 25$ mM, $c'_N = c''_N = 125$ mM, $U = 0$.

linearly related to c^a_{val} [60,61] in the following way

$$P_K = a_K c^a_{val} + b_K \tag{14}$$

$$P_N = a_N c^a_{val} + b_N \tag{15}$$

b_K and b_N account for the valinomycin-independent ion permeabilities of the vesicle membrane. The numerical simulations represented in Fig. 2 were carried out with the following parameter values: $a_K = 60\ M^{-1} \cdot cm \cdot s^{-1}$, $a_N = 0.09\ M^{-1} \cdot cm \cdot s^{-1}$, $b_K = 10^{-9}\ cm \cdot s^{-1}$ and $b_N = 8 \cdot 10^{-10}\ cm \cdot s^{-1}$. Similar values were used later for numerical fits to voltage signals observed in vesicle experiments.

It is seen from Fig. 2 that in the absence of valinomycin the voltage signal rises steeply, reflecting the electrogenic action of the pump. According to Eqn. 10, the initial slope of $U(t)$ is independent of valinomycin concentration and is given by

$$\left(\frac{dU}{dt}\right)_{t=0} \equiv H_0 = -\frac{e_0}{AC_m}(J_{N,p} + J_{K,p}) \tag{16}$$

Eqn. 16 is obtained from Eqn. 10 by introducing the conditions $u = 0$, $c'_N = c''_N$ and $c'_K = c''_K$ at $t = 0$. At finite valinomycin concentrations c^a_{val}, the fast initial rise is followed by a slower voltage increase resulting from the quasistationary build-up of a K^+-concentration gradient. At large values of c^a_{val}, the initial slope predicted by Eqn. 16 is only marginally visible. In the limit of large c^a_{val}, the membrane voltage U approaches the Nernst potential E_K for potassium

$$U \approx E_K = \frac{RT}{F} \ln \frac{c''_K}{c'_K} \tag{17}$$

For $c^a_{val} \to \infty$ the membrane is short-circuited by the high K^+-permeability, so that the net inward flow of charge through the pump, $-e_0(J_{N,p} + J_{K,p})$, is compensated by a valinomycin-mediated efflux of K^+. This means that the relation $J_{N,p} + J_{K,p} = J_{K,v}$ holds. Under this condition Eqn. 9 reduces to

$$-V_i \frac{dc'_K}{dt} = J_{N,p} \tag{18}$$

From Eqn. 17 the rate of voltage change at high valinomycin concentration is given by $dU/dt = -(RT/Fc'_K)\ dc'_K/dt$ (since c''_K is nearly constant). Together with Eqn. 18 one obtains

$$\frac{dU}{dt} \approx -\frac{RT}{F}\frac{J_{N,p}}{V_i c'_K} \tag{19}$$

This equation holds for times t larger than the brief charging time $\tau_c = C_m/\lambda_t \approx C_m/\lambda_k = RTC_m/F^2 P_K c''_K$. At a potassium concentration of 50 mM and a valinomycin concentration of 1 nM, λ_K may be estimated to be about 3 $\mu S/cm^2$ for $a_k = 60\ M^{-1} \cdot cm \cdot s^{-1}$ yielding (with $C_m \approx 1\ \mu F/cm^2$) $\tau_c \approx 0.3$ s. This means, since τ_c is of the same order or smaller as the mixing time after addition of ATP, that the true initial slope of U predicted by Eqn. 16 is barely visible at valinomycin concentrations larger than about 1 nM. Instead, from $U(t)$ an apparent 'initial' slope H_∞ for large valinomycin concentration ($c^a_{val} \to \infty$) is obtained by extrapolating dU/dt from times $t > \tau_c$ back to $t = 0$ (compare Fig. 2). Inserting the initial concentration $c'_K(t = 0) = c'_{K,0}$ into Eqn. 19, the extrapolated initial slope of $U(t)$ becomes

$$\left(\frac{dU}{dt}\right)_{t \to 0} \equiv H_\infty = -\frac{RT}{F}\frac{J_{N,p}}{V_i c'_{K,0}} \quad (c^a_{val} \to \infty) \tag{20}$$

According to Eqns. 16 and 20, the coupling ratio ρ_{NK} is given by

$$\rho_{NK} \equiv -\frac{J_{N,p}}{J_{K,p}} = \left(1 - \frac{1}{c'_{K,0} V_i Q} \cdot \frac{H_0}{H_\infty}\right)^{-1} \tag{21}$$

Eqn. 21 relates the coupling ratio ρ_{NK} to the experimental quantities H_0 and H_∞ which are given by the initial slopes of $U(t)$ at vanishing and at high valinomycin concentration, respectively. Since the accurate determination of initial slopes may be difficult, it is sometimes preferable evaluating ρ_{NK} by fitting Eqns. 10–12 to a more extended portion of $U(t)$ in the vicinity of $t = 0$. The fitting procedure which has been used for the

analysis of the experimental results also accounts for vesicle heterogeneity, as will be discussed in the following.

Influence of vesicle heterogeneity

Since vesicle formation and incorporation of protein molecules by detergent dialysis is a stochastic process, the resulting vesicle population is heterogeneous with respect to vesicle diameter and number of outward-oriented pumps per vesicle. A vesicle with a large number n of functional pumps will exhibit a faster rise of voltage than vesicles with smaller n. To account for vesicle heterogeneity in the analysis of optical signals, the following method can be used [62]. We assume that the vesicle radii approximately exhibit a Gaussian distribution $\rho(r)$ with mean radius $\bar{r}$ and half-width σ:

$$\rho(r) = \frac{1}{\sqrt{2\pi}\sigma} \exp\left(-\frac{(r-\bar{r})^2}{2\sigma^2}\right) \tag{22}$$

$$\sigma^2 = \overline{(r-\bar{r})^2} \tag{23}$$

We further assume that the number n of functionally-oriented pump molecules in a vesicle obeys a Poisson distribution and that the average value of n is proportional to the area $A = 4\pi r^2$ of the vesicle membrane. The assumption of a Poisson distribution is supported by a recent statistical analysis of electron-microscopic pictures of reconstituted vesicles [63]. The probability $P(n, r)$ that a vesicle of radius r contains n functionally oriented pumps is equal to

$$P(n, r) = \frac{(\bar{n})^n \exp(-\bar{n})}{n!} \tag{24}$$

$$\bar{n}(r) = 4\pi r^2 \chi$$

χ is the average surface density of outward-oriented pump molecules.

The observed fluorescence intensity F (corrected for the small background fluorescence of oxonol dissolved in the aqueous phase) can be represented as the sum of contributions of individual vesicles. In the following, we denote the contribution of the j-th vesicle to $F(t)$ by f_j and the value of f_j at voltage $U = 0$ by f_{j0}. The ratio f_j/f_{j0} is then a well-defined function of U which may be determined by calibration [53]:

$$\frac{f_j}{f_{j0}} = w(U_j) \tag{25}$$

The experimental quantity of interest is the ratio $S(t) = F(t)/F_0$, where F_0 is the value of F at zero voltage. $S(t)$ is given by

$$S(t) = \frac{1}{F_0}\sum_j f_j(t) = \frac{1}{F_0}\sum_j f_{j0}\, w[U_j(t)] \tag{26}$$

The ratio f_{j0}/F_0 is equal to A_j/A_t, where A_j is the surface area of the j-th vesicle and A_t the total surface area of the suspension. Thus,

$$S(t) = \frac{1}{A_t}\sum_j A_j\, w[U_j(t)] \tag{27}$$

To carry out the summation in Eqn. 27, the vesicle population is subdivided into discrete classes. For instance, class (k,n) contains all vesicles with radii between r_k and $r_k + \Delta r$ having exactly n functionally-oriented pumps. The number of vesicles in each class is given by Eqns. 22 and 24. With $A = 4\pi r_k^2$, Eqn. 27 then becomes

$$S(t) = \frac{4\pi}{A_t}\sum_n\sum_k P(n, k) r_k^2 \rho(r_k)\, w[U(k, n, t)]\, \Delta r_k \tag{28}$$

For the evaluation of $S(t)$, $U(k, n, t)$ is calculated as a function of time t for given values of n and k by numerical integration of Eqn. 10 or Eqn. A-7.

Results

Response time of the potential-sensitive dye

Previous studies of the mechanism of voltage-induced fluorescence changes of oxonol VI indicate that creation of an inside-positive potential leads to uptake of the anionic dye into the intravesicular space and to enhanced partitioning into the lipid membrane [53,64–67]. A prerequisite for an accurate measurement of time-dependent voltage changes is a sufficiently short response time of the dye. In experiments with bacterial chromatophores, oxonol VI was found to respond in the time range of milliseconds to light-induced changes of membrane potential [64]. In order to get information on the response time under the conditions of our vesicle studies, we have carried out a series of stopped-flow experiments. In these experiments which will be described in detail elsewhere [69], a suspension of vesicles equilibrated with oxonol VI, valinomycin and 2.5 mM K_2SO_4 was rapidly mixed with a 75 mM K_2SO_4 solution. In this way a Nernst potential for K^+ of about 66 mV was generated within ≈ 10 ms. After mixing, a fluorescence increase exhibiting a nearly exponential time-course with a time constant τ of about 290 ms was observed. Since τ is shorter than the rise time of the fluorescence signal in the experiments with reconstituted Na^+/K^+-ATPase (see below), effects of the finite response time of the dye are small. In the analysis of the experimental results, the influence of finite response time has been accounted for by the method described in Appendix A.

Fluorescence signals associated with pump activity

The time-course of fluorescence intensity in an experiment with reconstituted lipid vesicles containing

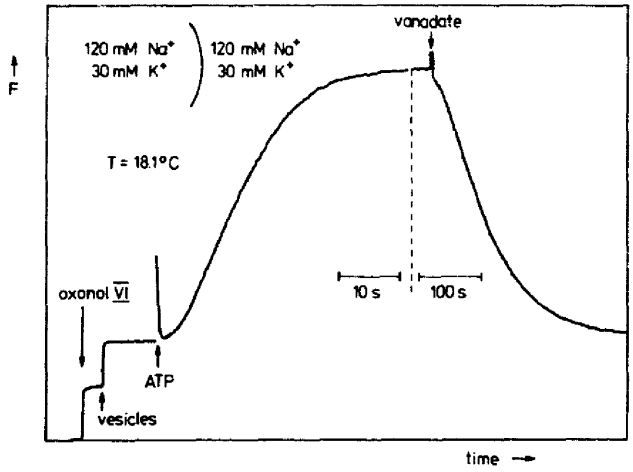

Fig. 3. Fluorescence signal associated with the generation of an inside-positive membrane potential after activation of the Na^+/K^+ pump. 30 nM oxonol, vesicles (8 $\mu g/cm^3$ lipid), 250 μM ATP and 2 mM vanadate were successively added to buffer H containing 120 mM Na^+ and 30 mM K^+. The vesicles were prepared with buffer H containing 120 mM Na^+ and 30 mM K^+. F is the fluorescence intensity. The temperature was 18.1° C. The average number of pump molecules per vesicle with outward-facing ATP-binding site was approximately 4.5.

Na^+/K^+-ATPase is represented in Fig. 3. After addition of vesicles to a solution of oxonol VI in buffer, the fluorescence increases as a result of dye binding to the lipid [53]. Activation of outward-oriented pump molecules by addition of ATP to the medium leads to a time-dependent fluorescence increase, corresponding to the generation of an inside-positive membrane potential [53]. As shown previously [53,64–67], this fluorescence increase results from increased partitioning of negatively-charged dye molecules into the inner leaflet of the lipid bilayer. When the pump is inhibited by addition of vanadate, the fluorescence decreases with a nearly exponential time-course (Fig. 3). From the time constant τ of the fluorescence decay and from the specific membrane capacitance $C_m \approx 1\ \mu F/cm^2$, the specific leakage conductance $\lambda = C_m/\tau$ may be estimated. After correcting for backtransport of charged dye molecules, λ is found to be approximately 15 nS/cm^2 under the experimental conditions of Fig. 3.

Fluorescence signals have been measured at different extravesicular concentrations of Na^+ (10–75 mM) and valinomycin ($c_{val} = 0$–50 nM). Examples are represented in Figs. 4 and 5 in which the average transmembrane voltage U_{av} is plotted as a function of time t after addition of ATP to the medium, U_{av} was evaluated from the fluorescence signal $S(t) = F(t)/F_0$ (compare Fig. 3), using the independently-determined fluorescence vs. voltage calibration. The calibration curve was obtained from experiments in which a Nernst potential for K^+ was generated in the presence of valinomycin and a K^+-concentration gradient, as described previously [53]. The voltage U_{av} determined in this way

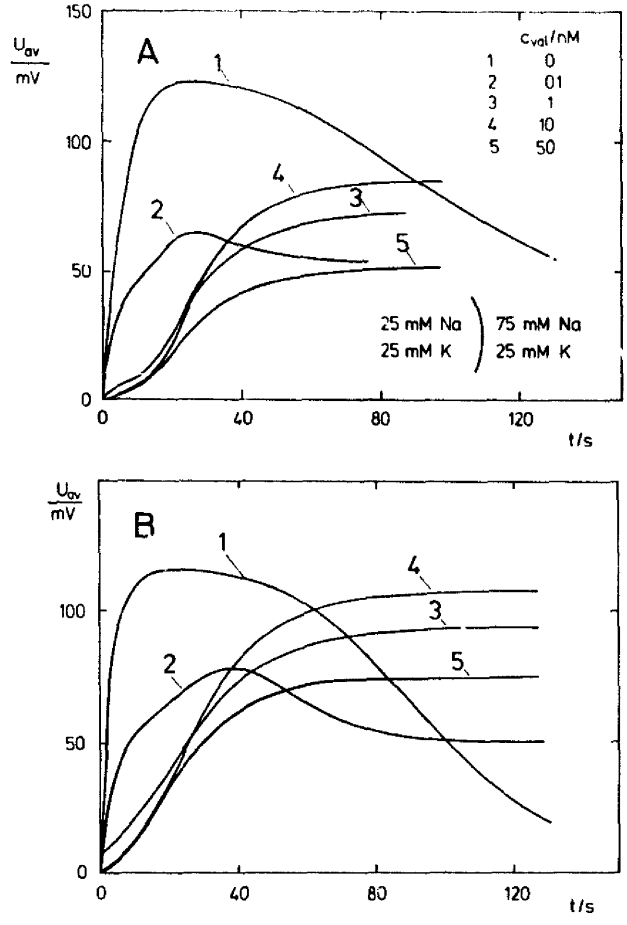

Fig. 4. (A) Transmembrane voltage $U_{av}(t)$ after addition of 0.5 mM Mg-ATP to the vesicle suspension at time $t = 0$ (compare Fig. 3). U_{av} is the apparent voltage which is evaluated from the fluorescence signal $S(t) \equiv F(t)/F_0$ using the fluorescence vs. voltage calibration carried out separately (see text). U_{av} represents an average over the vesicle population. Reconstituted vesicles were prepared by cholate dialysis for 60 h against buffer H containing 125 mM Na^+ and 25 mM K^+ (as sulfates). Thereafter the vesicles were equilibrated with buffer H containing 100 mM choline$^+$, 25 mM Na^+ and 25 mM K^+ (as sulfates) by dialysis for further 48 h. Choline was used to keep the ionic strength constant. In separate control experiments using ^{14}C-labeled sulfate, choline was found to equilibrate with the vesicle interior within a few hours. The two-stage procedure for the inclusion of choline was necessary since choline inactivated the enzyme when added prior to vesicle formation. Vesicles (final concentration about 6.6 mg lipid per cm^3) were diluted into buffer H containing 25 mM K^+, 75 mM Na^+ and 50 mM choline$^+$. The concentration of oxonol VI was 30 nM. c_{val} is the total concentration of valinomycin in the vesicle suspension; at a lipid concentration of 10 $\mu g/cm^3$, the free aqueous valinomycin concentration may be estimated to be about $0.91 \cdot c_{val}$ [60]. The temperature was 22° C.

(B) Numerical simulations of U_{av} for the same experimental conditions as in part (A) of the figure. The simulated curves were obtained from Eqns. 11, 12, 14, 15, A-7, A-10 and 28 with the following parameter values: $V_i = (4\pi/3)r_i^3$, $A = 4\pi r r_i$, $r_i = 44$ nm, $r = 48$ nm, $a_K = 60\ cm \cdot M^{-1} \cdot s^{-1}$, $a_N = 0.09\ cm \cdot M^{-1} \cdot s^{-1}$, $b_K = 10^{-9}\ cm \cdot s^{-1}$, $b_N = 8 \cdot 10^{-10}\ cm \cdot s^{-1}$, $\lambda = 2\ nS \cdot cm^{-2}$, $C_m = 1.0\ \mu F \cdot cm^{-2}$, $k_0 = 1/(2\tau) = 0.34\ s^{-1}$, $\beta = 5 \cdot 10^{-3}$ cm, $c = 30$ nM, $p = 0.9$, $c_{val}^a = 0.91\ c_{val}$, $\bar{r} = 48$ nm, $\sigma = 10$ nm, $\Delta r = 4.6$ nm, $\bar{n} = 4.5$, $v = 5.8\ s^{-1}$. The initial conditions ($t = 0$) were: $c_N' = 25$ mM, $c_N'' = 75$ mM, $c_K' = c_K'' = 25$ mM, $u = 0$. For the conversion of $S(t)$ (Eqn. 28) into $U_{av}(t)$, the independently determined calibration curve was used (Ref. 53).

represents an average over the vesicle population, since individual vesicles differ in size and in the number of pump molecules and therefore exhibit different rates of voltage change. For the moment, U_{av} may be considered as a phenomenological quantity for the representation of the experimental results; it will be discussed later how information on the ion fluxes $J_{N,p}$ and $J_{K,p}$ can be obtained from the time-course of U_{av}.

It is seen from Fig. 4A that in the absence of valinomycin U_{av} exhibits a fast rise towards a maximal value, followed by a slower decline. This decline results from the decrease of intravesicular potassium concentration, as K^+ is extruded after activation of the pump. A similar time-course of U_{av} is observed in the presence of valinomycin, but with a slower rise. This has to be expected, since in the absence of valinomycin the voltage rise results from the electrogenic effect of the pump, whereas at high valinomycin concentration, the voltage is determined by the Nernst potential for K^+ and reflects the slow change of intravesicular K^+ concentration. In the limit of large valinomycin concentration c_{val}, the slope of U_{av} at $t = 0$ becomes independent of c_{val}. This behaviour of U_{av} is more clearly seen from Fig. 5 in which U_{av} is plotted for small values of t on an expanded scale.

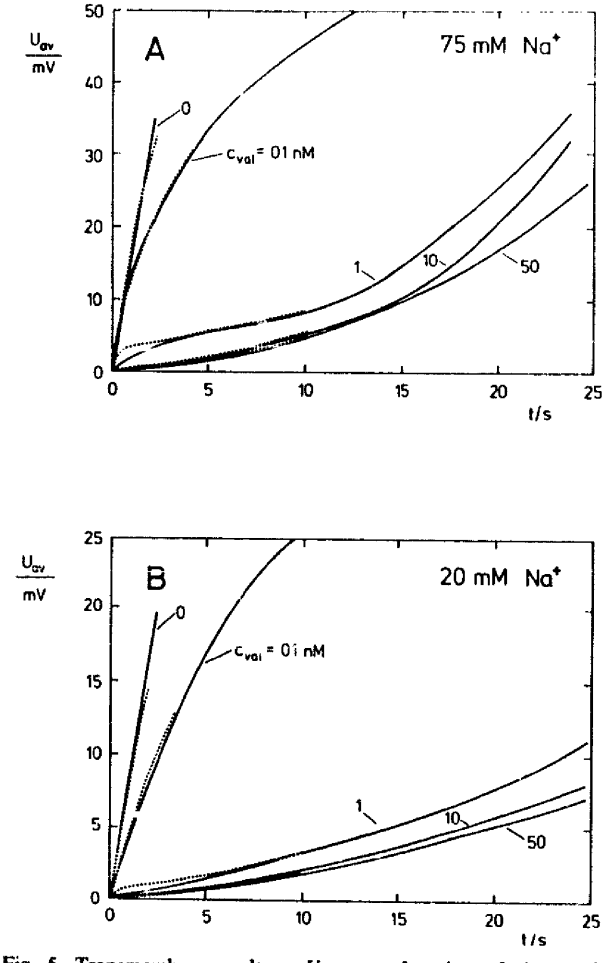

Fig. 5. Transmembrane voltage U_{av} as a function of time t for different concentrations of valinomycin (0, 0.1, 1, 10 and 50 nM). The initial ionic concentrations were: $c'_N = c''_N = 75$ mM, $c'_K = c''_K = 25$ mM (A) and $c'_N = c''_N = 20$ mM, $c'_K = c''_K = 25$ mM (B). The total concentration of ($K^+ + Na^+ +$ choline$^+$) was 150 mM. The other experimental conditions were the same as in Fig. 4A. Fig. 5A is replotted from Fig. 4A at a different time-scale. The dotted lines have been obtained by numerical simulation using the parameter values given in the legend of Fig. 4, except for $b_K = 6 \cdot 10^{-9}$ cm·s^{-1}, $b_N = 6 \cdot 10^{-10}$ cm·s^{-1}.

TABLE I

Initial slopes H_0 and H_∞ of transmembrane voltage (Eqns. 16 and 20) and coupling ratio $\rho_{NK} = -J_{N,p}/J_{K,p}$ for different extravesicular sodium concentrations c''_N

Apart from c''_N, the experimental conditions were the same as described in the legend of Fig. 4. For the quantity $c'_{K,0}V_i Q$ in Eqn. 21, a value of 127 was used (see text). The error limits indicate the uncertainty in the determination of the initial slope (H_0 and H_∞) of U_{av}. The parameter values used in the simulation are given in the legend of Fig. 5.

c''_N (mM)	H_0 (mV/s)	H_∞ (mV/s)	H_0/H_∞	ρ_{NK}	
				from H_0/H_∞ (Eqn. 21)	by simulation
10	2.86	0.06	46 (±7)	1.57 (±0.24)	1.57
15	7.1	0.14	52 (±13)	1.69 (±0.43)	1.57
20	8.3	0.18	47 (±7)	1.57 (±0.24)	1.57
30	13.8	0.27	51 (±12)	1.67 (±0.41)	1.56
75	16.0	0.39	41 (±8)	1.48 (±0.29)	1.50

Values of the initial slopes, H_0 and H_∞, of $U_{av}(t)$ in the limits of zero and high valinomycin concentration are given in Table I for different extravesicular Na^+ concentrations c''_N. Both H_0 and H_∞ decrease with decreasing c''_N, reflecting the dependence of turnover rate on sodium concentration [52], but the ratio H_0/H_∞ remains nearly constant.

According to Eqn. 21, the coupling ratio $\rho_{NK} = -J_{N,p}/J_{K,p}$ may be evaluated from the experimental values of H_0/H_∞. The product $c'_{K,0}V_i$ in Eqn. 21 is the number of K^+ ions initially present in the intravesicular aqueous space. In previous light-scattering experiments [58], the average external radius of reconstituted Na^+/K^+-ATPase vesicles, prepared by cholate dialysis under similar conditions as in this study, has been determined to be $r \approx 48$ nm. Nearly the same value has been obtained from electron microscopy [70]. With a membrane thickness of $d = 4$ nm, the volume of the intravesicular space becomes $V_i = (4\pi/3)r_i^3 \approx 3.6 \cdot 10^{-16}$ cm^3, where $r_i = r - d = 44$ nm is the internal radius of the vesicle. In the experiments of Fig. 4, the initial K^+ concentration was the same inside and outside the vesicles and was equal to 25 mM. This gives $c'_{K,0} = c''_K = 1.51 \cdot 10^{19}$ cm^{-3}, so that $c'_{K,0}V_i \approx 5370$. With a value of $A = 4\pi r r_i \cong 2.7 \cdot 10^{-10}$ cm^2 for the average membrane

area of a vesicle and with a specific capacitance of $C_m \approx 1.0\ \mu F/cm^2$, the quantity Q (Eqn. 13) becomes equal to 0.024, which yields $c'_{K,0} V_i Q = 127$. Values of the coupling ratio ρ_{NK} which are obtained in this way are given in Table I. ρ_{NK} is found to be close to 1.5, i.e., close to the value predicted for a pump with a stoichiometry of 3 Na^+ : 2 K^+ operating with fully occupied binding sites.

The values of ρ_{NK} given in Table I are subjected to uncertainties resulting from errors in the determination of the initial slope of $U_{av}(t)$. The error introduced in this way is largest at low Na^+ concentrations where H_∞ is small. Absolute error limits corresponding to the uncertainty in the slope of U_{av} are given in Table I together with the values of H_0, H_∞ and ρ_{NK}. Other errors result from the estimated average vesicle radius which is required for the evaluation of the quantities $V_i \propto r_i^3$ and $Q = e_0 F/RTAC_m \propto 1/r r_i$ in Eqn. 21. However, since QV_i is approximately proportional to the first power of r_i, errors in the vesicle radius influence the value of ρ_{NK} only weakly. More serious sources of error consist in the heterogeneity of the vesicle population and in the effects of charge transport associated with voltage-induced redistribution of dye molecules. Accounting for these error sources requires numerical integration of the rate equations, as will be discussed in the next section.

Analysis of fluorescence signals

A more accurate evaluation of the coupling ratio ρ_{NK} is possible by fitting the rate equations derived in the theoretical part of the paper to the experimentally observed fluorescence signals. For this purpose, Eqn. 10 which is independent of the nature of the voltage-sensitive dye has to be modified by addition of a term describing the contribution of oxonol VI redistribution to the overall charge translocation across the vesicle membrane. The necessity for such a correction term can be seen in the following way.

If pump molecules translocate Δn_q net charges across the vesicle membrane, a transmembrane voltage $\Delta U = e_0 \Delta n_q / AC_m$ is built up. Since the negatively-charged oxonol molecules distribute between intravesicular aqeous space and external medium according to a Nernst equilibrium [53], the relation $\Delta U = (RT/F)\ln[(c + \Delta c)/c]$ holds, where c and $c + \Delta c$ are the extra- and intravesicular aqueous concentrations of the dye. Accordingly, for small Δn_q, Δc is equal to $c[\exp(F\Delta U/RT) - 1] \approx F\Delta U/RT = Qc\Delta n_q$. Denoting the interfacial concentrations (cm^{-2}) of adsorbed dye molecules at the outer and the inner leaflet of the membrane by N and $N + \Delta N$, respectively, the increment ΔN is given by $\Delta N = \beta \Delta c$, where β is the partition coefficient of the dye. Since for the establishment of the Nernst equilibrium, $\Delta n = A\Delta N + V_i \Delta c = (A\beta + V_i)\Delta c$ dye molecules must cross the membrane, the relation $\Delta n / \Delta n_q = Q(A\beta + V_i)c$ holds. With $Q = 0.024$, $r_i = 44$ nm, $A = 4\pi r r_i$, $V_i = (4\pi/3) r_i^3$ and $\beta = 5 \cdot 10^{-3}$ cm [53], the ratio $\Delta n / \Delta n_q$ becomes about 0.6 for an aqueous dye concentration of $c = 30$ nM. This means that dye redistribution is not negligible under the given experimental conditions.

The modification of Eqn. 10 required to account for charge translocation by the dye is described in Appendix A. The treatment given in Appendix A also accounts for the equilibration time of oxonol VI, which was determined to be about 300 ms from stopped-flow experiments [69]. The finite rate of dye translocation slows down the rise of the fluorescence signal. Numerical simulations show, however, that the effect is small under the conditions of our experiments, even at the highest rates of voltage change which are observed at vanishing valinomycin concentration.

The analysis of the observed fluorescence signals was based on a numerical integration of Eqns. 11, 12, A-7 and A-10. These equations specify the time-dependent quantities $c'_N(t)$, $c'_K(t)$, $u(t)$ and $y(t)$. The integration was carried out for each vesicle class $(k.n)$ separately, using fixed values of the parameters χ, r and σ which have been determined independently [51]. The fluorescence signal $S(t) = F(t)/F_0$ was calculated by summation over all vesicle classes according to Eqn. 28.

Since in the course of the experiment the transmembrane voltage U as well as the intravesicular K^+ concentration c''_K change with time, the dependence of turnover rate on U and c''_K has to be taken into account. This was done in the following way. The pump-mediated potassium flux $J_{K,p}$ was assumed to be dependent on c''_K according to a linear Michaelis-Menten relation

$$J_{K,p} = J_{K,p}^{max} \cdot \frac{c''_K}{c''_K + K_m} \tag{29}$$

The K_m value was assumed to be 0.1 mM [51]. To account for the voltage dependence of $J_{N,p}$ and $J_{K,p}$, the previously determined current-voltage characteristic of the pump in reconstituted vesicles [55] was used. This procedure represents only an approximate treatment of the voltage- and K^+-concentration dependence of the turnover rate. However, for the evaluation of $J_{N,p}$ and $J_{K,p}$ only the early phase of the fluorescence signal has been used during which c''_K and U remain close to their initial values $c''_K = c'_{K,0}$ and $U = 0$. For this reason the exact dependence of turnover rate on c''_K and U is of secondary importance. Since the extravesicular (cytoplasmic) sodium concentration was varied in different experiments, the initial turnover rate of the pump was adjusted to fit the initial slope of the voltage signal in the absence of valinomycin. The sodium concentration dependence of the turnover rate determined in this way agrees with the results of previous experiments with reconstituted proteoliposomes [52].

For the determination of the ion fluxes, estimated values of $J_{N,p}$ and $J_{K,p}$ were inserted into Eqns. 10–12, and in this way the time-dependent voltage $U(n, r_k, t)$ was predicted for a given class (n,k) of vesicles. Summation over all vesicle classes yields a predicted time-course $S(t)$ of the fluorescence signal which, in general, differed from the experimentally observed $S(t)$. Thereafter, new values of $J_{N,p}$ and $J_{K,p}$ were chosen, and the procedure was repeated until an approximate fit of the calculated signal to the experimental function $S(t)$ was obtained.

An example of a numerical integration is shown in Fig. 4B in which the time-course of U_{av} is simulated under the experimental conditions of Fig. 4A. It is seen that the simulated curves qualitatively agree with the experimental results. In particular, the observed decline of $U_{av}(t)$ at large t for low valinomycin concentrations is reproduced by the simulation. This decline results from a decrease of intravesicular (extracellular) K^+ concentration, leading to a decrease of turnover rate and a concomitant decay of transmembrane voltage through leakage pathways. At high valinomycin concentration, as K^+ ions are extruded from the vesicle, a Nernst potential for K^+ is built up. At large times, when the intravesicular K^+-concentration has become low and the Na^+ concentration high, the membrane potential is influenced by the permeabilities of both ion species (Na^+ and K^+).

In the simulations represented in Fig. 4B, no attempt has been made to obtain an optimal fit to the experimental $U_{av}(t)$ curves, since the fitting procedure becomes unreliable at large times. For a quantitative analysis, only the initial part of the signals has been used. The results of such simulations are shown in Fig. 5. The dashed lines in Fig. 5 have been obtained by adjusting $J_{N,p}$ and $J_{K,p}$ at each sodium concentration, keeping the other parameters (a_K, b_K, a_N, b_N, λ) constant. Values of $\rho_{NK} = -J_{N,p}/J_{K,p}$ determined by this way are represented in the last column of Table I. The ρ_{NK} values obtained by simulation agree within the limits of experimental error with the values determined from H_0/H_∞.

Discussion

In this paper we have described a method for studying the coupling ratio $\rho_{NK} \equiv -J_{N,p}/J_{K,p}$ of the Na^+/K^+-ATPase reconstituted in lipid vesicles. The method is based on a comparison of two transport rates, the rate of overall charge translocation (the pump current) and the rate of K^+ transport. A variant of this technique, consisting in the simultaneous measurement of pump current and sodium flux, has been used previously for studying the coupling ratio in nerve [71] and in muscle fibres [29,31]. In the reconstituted vesicle system, the evaluation of transport rates involves determination of the transmembrane voltage using potential-sensitive dyes. Since this requires calibration of the optical signal, the method is less direct than measurement of pump current and ion fluxes. The principal advantage of the optical technique is the much higher time-resolution (compared to conventional tracer-flux experiments) which allows the measurement of transport rates in the time range of seconds. An intrinsic complication of the reconstituted system lies in the fact that the vesicle population is heterogeneous with respect to vesicle diameter and number of functional pump molecules. As shown in this paper, effects of vesicle heterogeneity can be eliminated by taking the statistical properties of the vesicle population explicitly into account [62].

In the experimental range of cytoplasmic (extravesicular) sodium concentration (c_N'' between 10 and 75 mM), the coupling ratio ρ_{NK} was found to be constant and close to 1.5. This result agrees with previous estimates of ρ_{NK} from isotope-flux studies with kidney Na^+/K^+-ATPase reconstituted in lipid vesicles [42,43]. Evidence for coupling ratios of ≈ 1.5 has been obtained for the Na^+/K^+ pump of erythrocytes [13,72–74], squid axon [75,81], muscle [27,76] and oocytes [78] at physiological ion concentrations. Other experiments with squid axon [19], muscle [27,30,31] and erythroctye membrane vesicles [79] have shown that the coupling ratio is not fixed, but varies with the concentrations of Na^+ and K^+. Studies with reconstituted vesicles and erythrocyte membrane vesicles indicate that at low cytoplasmic sodium concentrations, H^+ instead of Na^+ may be actively transported by the Na^+/K^+ pump [77,80]. Furthermore, several investigations have shown that in the absence of K^+, the Na^+/K^+ pump can carry out net transport of Na^+ at low rate [6].

Appendix A

Charge translocation associated with dye redistribution

The following analysis is based on the previous demonstration [53] that the anionic dye oxonol VI behaves as a lipophilic ion which partitions between water and membrane/solution interface [68]. Assuming that partition equilibrium always exists between interface and water, the interfacial concentrations N' and N'' of the dye at the inner and outer interface (Fig. 6) are given by

$$N' = \beta c'; \qquad N'' = \beta c'' \tag{A-1}$$

β is the partition coefficient and c' and the c'' are the aqueous dye concentrations. For simplicity, β is considered to be voltage independent; this assumption implies that the adsorption plane coincides with the dielectric boundary between lipid and water [53] and thus represents an approximation. Neglecting the small contribution of the vesicles to the total volume V of the suspen-

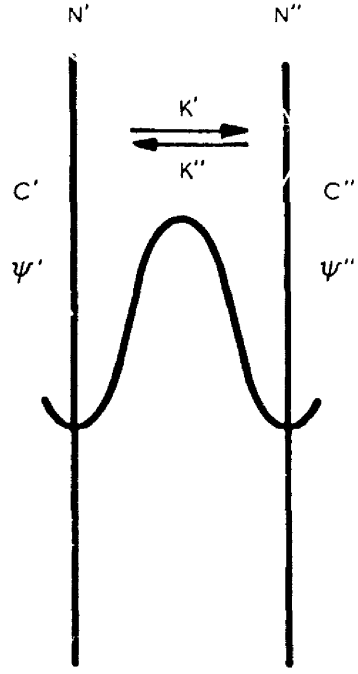

Fig. 6. Translocation of oxonol VI across the vesicle membrane. k' and k'' are the rate constants for crossing the central barrier, N' and N'' the interfacial concentrations of the dye, c' and c'' the aqueous dye concentrations and ψ' and ψ'' the electric potentials ($'$ intravesicular, $''$ extravesicular).

sion, the following relation holds for the total amount n_D of the dye:

$$n_D = c''V + n_v A(N' + N'') \tag{A-2}$$

n_v is the number of vesicles in the suspension and A the membrane area of a single vesicle. At equilibrium, prior to activation of the pump ($N' = N'' = N$, $c'' = c$), Eqn. A-2 assumes the form

$$n_D = cV + 2n_v AN \tag{A-3}$$

Combination of Eqns. A-1–A-3 yields

$$N'' = N(p+1) - pN' \tag{A-4}$$

$$p = \frac{\beta n_v A}{V + \beta n_v A} \approx \frac{\beta v_l}{d + \beta v_l} \tag{A-5}$$

v_l is the volume fraction of the lipid in the suspension and d the membrane thickness. With $\beta = 4.8 \cdot 10^{-3}$ cm [53], $d = 4$ nm and $v_l = 10^{-3}$ (corresponding to a lipid concentration of about 1 mg/cm^3), p becomes equal to 0.91.

The movement of dye molecules across the membrane may be described as a translocation over a symmetrical Eyring barrier [68]. Accordingly, the translocation rate constants k' and k'' (Fig. 6) are given by (with $u = F(\psi' - \psi'')/RT$)

$$k' = k_0 \exp(-u/2); \qquad k'' = k_0 \exp(u/2) \tag{A-6}$$

k_0 is the rate constant at zero voltage. The net outward flux of dye molecules across the membrane is equal to $k'N' - k''N'' = J$. The flux J represents a contribution $-e_0 AJ$ to the total transmembrane current, which has to be accounted for by the introduction of an additional term on the right side of Eqn. 10. Together with Eqn. A-1, the relation for the rate of voltage change then assumes the form

$$-\frac{du}{dt} = Q[\ ] + \frac{\lambda u}{C_m} - ay[\exp(-u/2) + p \cdot \exp(u/2)] + a(p+1)\exp(u/2) \tag{A-7}$$

$$a \equiv \frac{e_0 F k_0 \beta c}{RTC_m}; \qquad y \equiv \frac{N'}{N} \tag{A-8}$$

The symbol [ ] denotes the bracket in Eqn. 10. The time-dependent quantity y which appears in Eqn. A-7 may be obtained from the relation

$$\frac{dN'}{dt} = k''N'' - k'N' \tag{A-9}$$

(In this equation the small flux of dye into the intravesicular aqueous space is neglected). Introduction of Eqn. A-4 yields

$$\frac{dy}{dt} = -k_0 y[\exp(-u/2) + p \cdot \exp(u/2)] + k_0(p+1)\exp(u/2) \tag{A-10}$$

Eqns. 11, 12, A-7 and A-10 represent a system of coupled differential equations for the evaluation of the functions $c'_N(t)$, $c'_K(t)$, $u(t)$ and $y(t)$.

Acknowledgements

We would like to thank Milena Roudna and Renate Riek for expert technical assistance. This work has been financially supported by the Deutsche Forschungsgemeinschaft (Sonderforschungsbereich 156). R.J.C. acknowledges with gratitude financial support from the Alexander-von-Humboldt-Stiftung.

References

1 Skou, J.C. (1975) Q. Rev. Biophys. 7, 401–431.
2 Robinson, J.D. and Flashner, M.S. (1979) Biochim. Biophys. Acta 549, 145–176.
3 CantLey, L.C. (1981) Curr. Top. Bioenerg. 11, 201–202.
4 Schuurmans Stekhoven, F.M.A.H. and Bonting, S.L. (1981) Physiol. Rev. 61, 1–76.
5 Jørgensen, P.L. and Andersen, J.P. (1988) J. Membr. Biol. 103, 95–120.
6 Glynn, I.M. (1985) in The Enzymes of Biological Membranes (Martonosi, A.N., ed.), 2nd Edn. Vol. 3, pp. 35–114, Plenum Press, New York.
7 Kaplan, J.H. (1985) Annu. Rev. Physiol. 47, 535–541.

8 Thomas, R.C. (1972) Physiol. Rev. 52, 563–594.
9 Glynn, I.M. (1984) in Electrogenic Transport: Fundamental Principles and Physiological Implications (Blaustein, M.P. and Lieberman, M., eds.), pp. 33–48, Raven Press, New York.
10 De Weer, P., Gadsby, D.C. and Rakowski, R.F. (1988) Annu. Rev. Physiol. 50, 225–241.
11 De Weer, P., Gadsby, D.C. and Rakowski, R.F. (1988) in The Na^+,K^+-Pump, Part A: Molecular Aspects, Progress in Chemical and Biological Research, Vol. 268A, pp. 421–434, A.R. Liss, New York.
12 Post, R.L. and Jolly, P.C. (1957) Biochim. Biophys. Acta 25, 118–128.
13 Sen, A.K. and Post, R.L. (1964) J. Biol. Chem. 239, 345–352.
14 Garrahan, P.J. and Glynn, I.M. (1967) J. Physiol. (Lond.) 192, 217–235.
15 Funder, J. and Wieth, J.O. (1967) Acta Physiol. Scand. 71, 113–124.
16 Sachs, J.R. (1972) J. Clin. Invest. 51, 3244–3247.
17 Brinley, F.J. and Mullins, L.J. (1968) J. Gen. Physiol. 52, 181–211.
18 Baker, F.J., Blaustein, M.P., Keynes, R.D., Manil, J., Shaw, I.I. and Steinhardt, R.A. (1969) J. Physiol. (Lond.) 200, 459–496.
19 Mullins, L.J. and Brinley, F.J. (1969) J. Gen. Physiol. 53, 704–740.
20 Brinley, F.J. and Mullins, L.J. (1974) Ann. N.Y. Acad. Sci. 242, 406–433.
21 Abercrombie, R.F. and De Weer, P. (1978) Ann. J. Physiol. 235, C63–C68.
22 Rakowski, R.F. and De Weer, P. (1982) J. Gen. Physiol. 80, 25a.
23 Mullins, L.J. and Noda, K. (1963) J. Gen. Physiol. 47, 117–132.
24 Cross S.R., Keynes, R.D. and Rybová, R. (1965) J. Physiol. (Lond.) 181, 865–880.
25 Mullins, L.J. and Awad, M.Z. (1965) J. Gen. Physiol. 48, 761–775.
26 Adrian, R.H. and Slayman, C.L. (1966) J. Physiol. (Lond.) 184, 970–1014.
27 Sjodin, R.A. and Ortiz, O. (1975) J. Gen. Physiol. 66, 269–286.
28 Sjodin, R.A. (1982) J. Membr. Biol. 68, 161–178.
29 Lederer, W.J. and Nelson, M.T. (1984) J. Physiol. (Lond.) 348, 665–677.
30 Marunaka, Y. (1986) J. Membr. Biol. 91, 155–172.
31 Marunaka, Y. (1988) J. Membr. Biol. 101, 19–31.
32 Gadsby D.C. and Cranefield, P.F. (1979) Proc. Natl. Acad. Sci. USA 76, 1783–1787.
33 Eisner D.A. and Lederer, W.J. (1980) J. Physiol. (Lond.) 303, 441–474.
34 Glitsch, H.G., Pusch, H., Schumacher, T. and Verdonck, F. (1982) Pflügers Arch. 394, 256–263.
35 Nielsen, R. (1979) J. Membr. Biol. 51, 161–184.
36 Nielsen, R. (1979) Acta Physiol. Scand. 107, 189–191.
37 Glynn, I.M. and Karlish, S.J.D. (1976) J. Physiol. (Lond.) 256, 456–496.
38 Lee, K.H. and Blostein, R. (1980) Nature (Lond.) 285, 338–339.
39 Forgac, M. and Chin, G. (1982) J. Biol. Chem. 257, 5652–5655.
40 Cornelius, F. and Skou, J.C. (1985) Biochim. Biophys. Acta 818, 211–221.
41 Anner, B.M., Lane, L.K., Schwartz, A. and Pitts, B.J.R. (1977) Biochim. Biophys. Acta 467, 340–345.
42 Goldin, S.M. (1977) J. Biol. Chem. 252, 5630–5642.
43 Karlish, S.J.D. and Pick, U. (1981) J. Physiol. (Lond.) 312, 505–529.
44 Yoda, A., Clark, A.W. and Yoda, S. (1984) Biochim. Biophys. Acta 778, 332–340.
45 Anner, B.M. (1985) Biochim. Biophys. Acta 822, 319–334.
46 Anner, B.M. (1985) Biochim. Biophys. Acta 822, 335–353.
47 Cornelius, F. and Skou, J.C. (1987) Biochim Biophys Acta 904, 353–364
48 Cantley, L.C., Carilli, C.T. Smith, R.L. and Perlman, D. (1984) Curr. Top. Membr. Transp. 19, 315–322.
49 Anner, B.M. and Moosmayer, M. (1982) J. Membr. Sci. 11, 27–37.
50 Forbush III, B. (1984) Anal. Biochem. 140, 495–505.
51 Apell, H.-J., Marcus, M.M., Anner, B.M., Oetliker, H. and Läuger, P. (1985) J. Membr. Biol. 85, 49–63.
52 Apell, H.-J. and Marcus, M.M. (1986) Biochim. Biophys. Acta 862, 254–264.
53 Apell, H.-J. and Bersch, B. (1987) Biochim. Biophys. Acta 903, 480–494.
54 Goldschlegger, R., Karlish, S.J.D., Rephaeli, A. and Stein, W.D. (1987) J. Physiol. (Lond.) 387, 331–357.
55 Apell, H.-J. and Bersch, B. (1988) in The Na^+,K^+-Pump, Part A: Molecular Aspects, Progress in Chemical and Biological Research, Vol. 268A, pp. 469–476, A.R. Liss, New York.
56 Jørgensen, P.L. (1974) Methods Enzymol. 32, 277–290.
57 Anner, B.M., Marcus, M.M. and Moosmayer, M. (1984) in Enzymes, Receptors and Carriers of Biomembranes (Azzi, A., Brodbeck, U. and Cahler, P., eds.), pp. 81–99, Springer Verlag, Heidelberg.
58 Marcus, M.M., Apell, H.-J., Roudna, M., Schwendener, R.A., Weder, H.-G. and Läuger, P. (1986) Biochim. Biophys. Acta 854, 270–278.
59 Goldman, D.E. (1943) J. Gen. Physiol. 27, 37–60.
60 Stark, G. and Benz, R. (1971) J. Membr. Biol. 5, 133–153.
61 Stark, G., Benz, R. and Läuger, P. (1975) in Biomembranes-Lipids, Proteins and Receptors (Burton, R.M. and Packer, L., eds.), pp. 145–166, BI-Science Publications Division, Webster Grovess, MO.
62 Apell, H.-J. and Läuger, P. (1986) Biochim. Biophys. Acta 861, 302–310.
63 Apell, H.-J. and Marcus, M.M. (1985) in The Sodium Pump (Glynn, I. and Ellory, C., eds.), pp. 475–480, The Company of Biologists, Ltd., Cambridge.
64 Bashford, C.L., Chance, B. and Prince, R.C. (1979) Biochim. Biophys. Acta 545, 46–57.
65 Bashford, C.L., Chance, B., Smith, J.C. and Yoshida, T. (1979) Biophys. J. 25, 63–85.
66 Beeler, T.J., Farmen, R.H. and Martonosi, A.N. (1981) J. Membr. Biol. 62, 113–137.
67 Krab, K., Van Walraven, J.S., Scholts, M.J.C. and Kraayenhof, R. (1985) Biochim. Biophys. Acta 809, 228–235.
68 Ketterer, B., Neumcke, B. and Läuger, P. (1971) J. Membr. Biol. 5, 225–245.
69 Clarke, R. and Apell, H.-J. (1989) in Reactions in Compartmental Liquids (Knoche, W., ed.), Springer, Berlin, in press.
70 Anner, B.A., Robertson, J.D. and Ting-Beall, H.P. (1984) Biochim. Biophys. Acta 773, 253–261.
71 Cooke, I.M., Le Blanc, G. and Tauc, L. (1974) Nature 251, 254–256.
72 Gardos, G. (1964) Experientia 20, 387.
73 Whittam, R. and Ager, M.E. (1965) Biochem. J. 97, 214–227.
74 Post, R.L., Albright, C.D. and Dayani, K. (1967) J. Gen. Physiol. 50, 1201–1220.
75 Hodgkin, A.L. and Keynes, R.D. (1955) J. Physiol. (Lond.) 128, 28–60.
76 Clausen, T. and Hansen, O. (1974) Biochim. Biophys. Acta 345, 387–414.
77 Hara, Y. and Nakao, M. (1986) J. Biol. Chem. 261, 12655–12658.
78 Schwartz, W. and Gu, Q. (1988) Biochim. Biophys. Acta 945, 167–174.
79 Blostein, R. (1983) J. Biol. Chem. 258, 12228–12232.
80 Polvani, C. and Blostein, R. (1988) J. Biol. Chem., 263, 16757–16763.
81 Rakowski, R.F., Gadsby, D.C. and DeWeer, P. (1989) J. Gen. Physiol., in press.